Journal of Nuclear Materials 386–388 (2009) 49–51

Contents lists available at ScienceDirect

Journal of Nuclear Materials

journal homepage: www.elsevier.com/locate/jnucmat

Atomistic calculation of elastic constants of alpha-iron containing point defects by means of magnetic interatomic potentials

S. Chiesa [a], P.M. Derlet [a,*], S.L. Dudarev [b], H. Van Swygenhoven [a]

[a] Paul Scherrer Institute, CH-5232 Villigen PSI, Switzerland
[b] EURATOM/UKAEA Fusion Association, Culham Science Centre, Oxfordshire OX14 3DB, UK

A B S T R A C T

The recently developed magnetic potential for ferromagnetic BCC Fe [S.L. Dudarev, P.M. Derlet, J. Phys. ondens. Mat. 17 (2005) 7097; P.M. Derlet, S.L. Dudarev, Prog. Mater. Sci. 52 (2007) 299] is used to investigate the change in the elastic constants of bcc α-Fe as a function of a concentration of interstitial and vacancy defects. The results are discussed in terms of experiment and current theoretical understanding.

1. Introduction

Ferritic–martensitic steels are the main candidate structural materials for future fusion reactors and advanced fission power plants, and the development of quantitative computer models is expected to play a major role in rationalizing experimental information on the microstructural evolution of these materials under neutron irradiation. The defect structures arising under irradiation conditions consist fundamentally of interstitials and vacancies which condense into interstitial and vacancy prismatic loop structures that can migrate, transform and coalesce. In particular, under ion or neutron irradiation at room temperature, ⟨1 1 1⟩ and ⟨1 0 0⟩ interstitial and vacancy defect loops have been observed [1]. The precise way in which such defects affect the elastic and plastic response of α-Fe is also of paramount interest, and the subject of considerable activity in the multi-scale modeling community [2].

In the present work, atomistic simulation is used to investigate how the bulk elastic constants of pure α-Fe change with increasing concentrations of interstitials or vacancies. How the effective elastic constants are calculated for a general population of defect structures remains a non-trivial problem [3]. Moreover the precise distributions of loop structures as a function of dosage and temperature would also need to be known for a quantitative comparison with experiment. For the present work, these issues are not addressed and instead only simple interstitial and vacancy structures that retain an effective macroscopic cubic symmetry are considered. The atomistic simulations are performed using the magnetic potential for α-Fe [4,5]. Such an empirical potential takes into account the ferromagnetic contribution to the bonding that is known to stabilize the BCC phase. In its parameterization, a broad range of bulk equilibrium properties have been used as well as *ab initio* derived single interstitial defect energies [6,7].

2. Method and results

To calculate the elastic constants of either an interstitial or vacancy defect structure in α-Fe, the chosen atomic configuration is affinely distorted and the internal coordinates are relaxed via a conjugate gradient energy minimization procedure. The elastic constants are then directly obtained by extracting the quadratic energy dependence as a function of the magnitude of the distortion [8]. For the bulk modulus an isotropic volume distortion is performed, for the $C' = (C_{11} - C_{12})/2$ elastic constant a volume conserving tetrahedral distortion is applied and for the C_{44} elastic constant a volume conserving shear on a (1 0 0) plane.

In the choice of an appropriate defect structure, one must take into account that under normal experimental circumstances, the macroscopic cubic symmetry of the irradiated material is maintained. That is, defect structures will in principle arrange themselves such to minimize long range stress fields to preserve the macroscopic BCC structure. A single ⟨1 1 0⟩ dumbbell interstitial does not have cubic symmetry and therefore an appropriate arrangement of interstitials is needed for the intended calculation. For the present work the simplest configuration is considered: a twelve interstitial atom defect structure in which initially twelve (two atom) split ⟨1 1 0⟩ dumbbells are set in an otherwise perfect bcc lattice at the locations (0,±2,±2), (±2,0,±2) and (±2,±2,0) (in units of the lattice constant) with their dumbbell axes perpendicular to their corresponding position vector. Prior to each series of distortions such atomic configurations are relaxed via the conjugate gradient method and the volumes adjusted to obtain a zero global hydrostatic pressures. The relaxed interstitial configuration

* Corresponding author.
E-mail address: peter.derlet@psi.ch (P.M. Derlet).

0022-3115/$ - see front matter © 2008 Elsevier B.V. All rights reserved.
doi:10.1016/j.jnucmat.2008.12.056

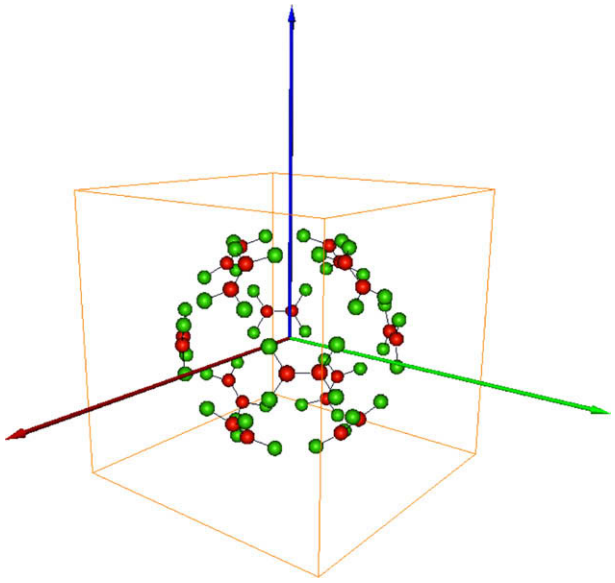

Fig. 1. A symmetric configuration of twelve ⟨1 1 0⟩ dumbbells in a simulation cell with a periodic side length of eight lattice constants. Only atoms with a potential energy higher −3.99 eV are visualized. The pairs of atoms constituting each dumbbell are colored in red and the axes indicate the ⟨1 0 0⟩ directions.

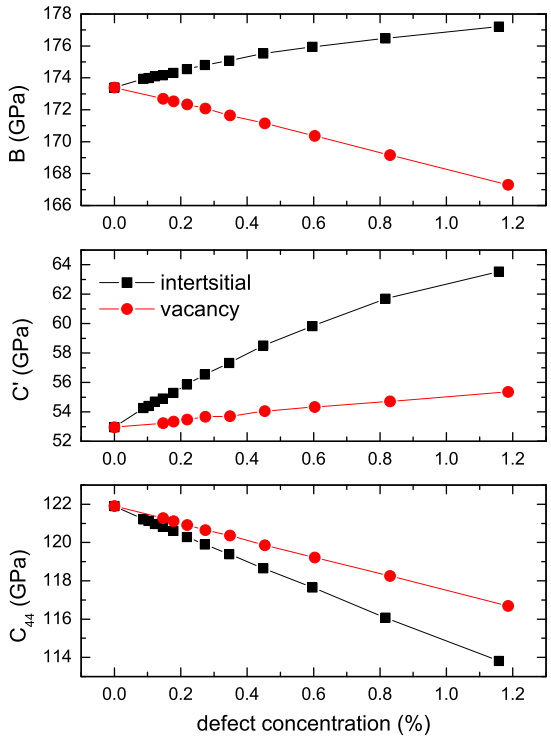

Fig. 2. The elastic constants as a function of interstitial and vacancy defect concentration.

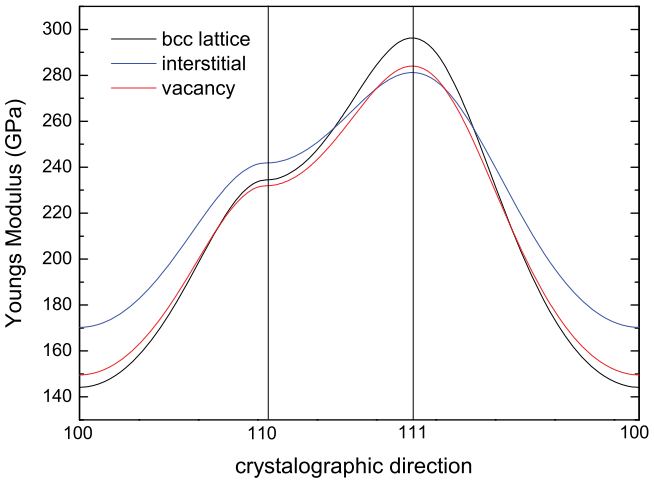

Fig. 3. Plot of the directional dependent Young's modulus along the 1 0 0 to 1 1 0 to 1 1 1 to 1 0 0 stereographic path.

is shown in Fig. 1, where atoms with local cohesive energies higher than that of the bulk BCC lattice are shown. The ⟨1 1 0⟩ dumbbell configurations are clearly evident in the 1 0 0 orientated simulation cell geometry. Although a vacancy defect does not break cubic symmetry, in the present work we consider also a twelve vacancy defect structure that is prepared in a similar fashion. To investigate the change in elastic constants as a function of interstitial and vacancy concentration, the simulation cell size is then varied while keeping the absolute positions of the ⟨1 1 0⟩ dumbbells and vacancies fixed. For the range of concentrations considered, the side length of the simulation cell is varied from eight (~3 nm) to eighteen (~5 nm) lattice constants.

Fig. 2 displays the corresponding elastic constants as a function of vacancy and interstitial defect concentration. For the interstitial defect, the bulk modulus and C' shear modulus increase with defect concentration, whilst the C_{44} shear modulus decreases. For the case of the vacancy defect, the shear moduli follow the same trend; however the bulk modulus is seen to decrease as a function of increasing vacancy concentration. Note that as a function of increasing concentration, the average volume per atom increases linearly for the interstitial defect and decreases linearly for the vacancy defect, suppressing the effects of bond stiffening/softening for the interstitial and enhancing them for the vacancy as a function of increasing concentration. Fig. 3 shows how the changes in the elastic constants are reflected in the directional dependency of the Young's modulus. In this graph, the horizontal axis represents a path starting from the 1 0 0 crystal loading direction that traverses the unit sphere to the 1 1 0 direction, then to the 1 1 1 direction and then finally returning to the 1 0 0 direction. This path is the boundary of the basic triangle in a stereographic projection for a cubic system. Inspection of the perfect lattice case indicates that the elastically softest direction is along the 1 0 0 axis whilst the elastically hardest is along the 1 1 1 direction. In terms of the Young's modulus which is neither a pure shear nor a pure isotropic distortion, the presence of either interstitial or vacancy defects results in a stiffening along the 1 0 0 direction (in part due to the stiffening of C') and a softening along the 1 1 1 direction (in part due to the softening of C_{44}). Along the 1 1 0 direction, the vacancies produce a softening and the interstitials a hardening.

3. Discussion and concluding remarks

The bulk modulus and C' elastic hardening seen in Fig. 2 appears to be at odds with both experiment and current theoretical understanding, both of which suggest that all elastic constants soften. For example, ultra sound measurements that probe both C' and C_{44} and performed as a function of Frenkel pair concentration c in α-Fe [9], observed a softening given by $\partial \ln C'/\partial c = -27 \pm 2$ and $\partial \ln C_{44}/\partial c = -17 \pm 4$. On the other hand Fig. 2 gives $\partial \ln C'/\partial c \approx 15$ and $\partial \ln C_{44}/\partial c \approx -6$. Such softening as a function of neutron irradiation has also been seen in the 1 0 0, 1 1 0 and 1 1 1 Young's moduli of tungsten and molybdenum [10]. Early work on the lattice theory of interstitial and vacancy point defects [11,12] revealed that the

vibrational spectrum of point defects may be characterized by low frequency resonance modes whose effect persists to the long wave length limit through a renormalization of the sound velocity. Indeed the data of Fig. 2 may be reproduced by diagonalizing the resulting Hessian of each undistorted configuration to obtain the long wave length dispersion curves, yielding the directionally dependent sound velocities and thus the configuration's elastic constants. Such resonance modes are intimately related to the mobility of the defect, since the existence of a migration barrier will lead to a reduction in the local force constants and an associated local softening. Dederichs et al. [12] demonstrate that this results in an induced positive internal stress that enhances the external stress associated with the imposed distortion, resulting in an effective reduction of the material's elastic constants.

The single interstitial or vacancy defects concentrations seen in Fig. 2 are high. To estimate the experimental concentration, consider a material with m $\langle 1\,1\,1\rangle$ loops per unit volume with a mean diameter d. Supposing the surface of the loop is composed of point defects and on the $\langle 1\,1\,1\rangle$ plane, the number of defects per unit area of the loop surface is given by $\sigma = a^2/\sqrt{3}$, where a is the lattice constant. Taking the total defect surface as a circle of diameter d, the number of defects per unit volume is then approximately given by $n = \pi d^2 m/4\sigma$. After neutron irradiation of pure iron at 100 C to 1 dpa, the density of clusters is $\sim 7 \times 10^{23}$ m^{-3} with a mean diameter of 4 nm [13]. Inserting these values into the last equation results in $\sim 2 \times 10^{25}$ interstitials per cubic meter corresponding to a defect concentration of $\sim$0.02%. Loop structures contain however defect core structures only around the perimeter of the interstitial or vacancy disk, whereas for the present simulations the concentration is with respect to point defects. Thus the contribution to the elastic constants arising from the core defect region is considerable and strong non-linear elastic effects can be expected – a regime that the current theoretical understanding does not address.

In light of the above considerations, the observed elastic stiffening in the bulk modulus and the tetrahedral shear modulus may be an artifact of the high concentrations of point defects used and/or the current parameterization of the magnetic potential. The former can only be addressed by considering large simulations cells containing realistic interstitial and vacancy defect structures such 1 1 0, 1 0 0 and 1 1 1 vacancy and prismatic loops, and the latter is currently being investigated through a study of the anharmonic properties of the magnetic potential.

References

[1] M.L. Jenkins, M.A. Kirk, W.J. Phythian, Journal of Nuclear Materials 205 (1993) 16;
S.L. Dudarev, R. Bullough, P.M. Derlet, Phys. Rev. Lett. 100 (2008) 135503.
[2] I. Cook, Nat. Mater. 5 (2006) 77.
[3] J.E. Gubernatis, J.A. Krumhansl, J. Appl. Phys. 46 (1975) 1875.
[4] S.L. Dudarev, P.M. Derlet, J. Phys.-Condens. Mat. 17 (2005) 7097.
[5] P.M. Derlet, S.L. Dudarev, Prog. Mater. Sci. 52 (2007) 299.
[6] C.C. Fu, F. Willaime, P. Ordejon, Phys. Rev. Lett. 92 (2004).
[7] D. Nguyen-Manh, S.L. Dudarev, A.P. Horsfield, J. Nucl. Mater. 367 (2007) 257.
[8] M.W. Finnis, Interatomic Forces in Condensed Matter, Oxford University, 2003.
[9] S.J. Zinkle, B.N. Singh, J. Nucl. Mater. 351 (2006) 269.
[10] B. Igarashi, E.C. Johnson, A.V. Granato, Phys. Rev. B 48 (1993) 2909.
[11] M.I. Zakharova, N.A. Artemov, V.V. Bogdanov, Inorg. Mater. 37 (2001) 786.
[12] P.H. Dederichs, C. Lehmann, H.R. Schober, A. Scholz, R. Zeller, J. Nucl. Mater. 69&70 (1978) 176.
[13] P.H. Dederichs, R. Zeller, Phys. Rev. B 14 (1976) 2314.